Excitons in topological Kondo insulators: Theory of thermodynamic and transport anomalies in SmB_6

Johannes Knolle* and Nigel R. Cooper
T.C.M. Group, Cavendish Laboratory, J.J. Thomson Avenue, Cambridge CB3 0HE, United Kingdom
(Received 3 November 2016; published 3 March 2017)

Kondo insulating materials lie outside the usual dichotomy of weakly versus correlated—band versus Mott—insulators. They are metallic at high temperatures but resemble band insulators at low temperatures because of the opening of an interaction-induced band gap. The first discovered Kondo insulator (KI) SmB_6 has been predicted to form a topological KI (TKI). However, since its discovery thermodynamic and transport anomalies have been observed that have defied a theoretical explanation. Enigmatic signatures of collective modes inside the charge gap are seen in specific heat, thermal transport, and quantum oscillation experiments in strong magnetic fields. Here, we show that TKIs are susceptible to the formation of excitons and magnetoexcitons. These charge neutral composite particles can account for long-standing anomalies in SmB_6.

DOI: 10.1103/PhysRevLett.118.096604

One of the biggest successes of quantum mechanics is the explanation of the distinction between metals and insulators. Traditionally, there are two different regimes: First, in weakly interacting systems insulating behavior arises from complete filling of Bloch bands with a gap to unoccupied states, whereas metals have partially filled bands giving a manifold of gapless excitations—the Fermi surface (FS). Second, in strongly interacting systems repulsion forbids hopping of electrons leading to Mott insulators. However, a third possibility exists—so-called Kondo insulators (KI)—where strong interactions between itinerant electrons and localized spins lead to a heavy band insulator at low temperatures [1].

The material SmB_6 was the first KI discovered almost half a century ago [2]. More recently, it has been predicted that SmB_6 should be a topological KI (TKI) [3] that is an interaction-induced heavy three-dimensional topological insulator [4]. Normally the charge gap in an insulator also determines its thermodynamic and bulk transport properties, which are expected to then follow an Arrhenius-type activated temperature dependence. However, the tentative TKI SmB_6 strongly deviates from that picture and exhibits unusual thermodynamic anomalies, for example, a low temperature specific heat contribution reminiscent of a metal [5,6]. These have not found a generally accepted explanation for decades and more recent experiments motivated from the TKI proposal have added even bigger puzzles. The observation of bulk quantum oscillations (QO) [7], normally a synonym for a FS, and residual thermal transport inside the insulating low temperature regime [8] challenge our canonical understanding of metals and insulators.

Here, we show that TKIs are very susceptible to the formation of excitons or magnetoexcitons (MEXC) in an applied magnetic field B. The strong Coulomb repulsion of the localized Sm f levels has two effects. First, it gives rise to a heavy insulating state with a peculiar broad-brimmed Mexican hatlike band structure, see Fig. 1, which provides the necessary large density of states (DOS) from the band extrema; see the right panel. Second, it provides the interaction that binds the particle-hole pairs. While spin excitons [9–11] have been discussed in connection with collective in-gap modes observed in inelastic neutron scattering (INS) [12–14] before, here we show that a new exciton branch at lower energies can provide a natural explanation of long-standing thermodynamic anomalies in SmB_6. In addition, by generalizing the theory of MEXC to TKIs we discover a new mechanism by which an insulator without a FS can exhibit bulk quantum oscillations.

The model.—We focus on a minimal model of a TKI that captures the essential physics of SmB_6 and takes the form of a periodic Anderson lattice model [3,15].

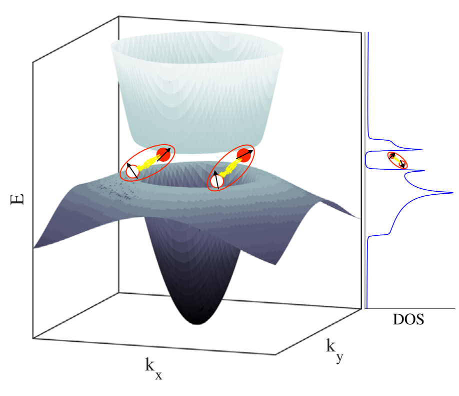

FIG. 1. At low temperatures strong correlations lead to the formation of fermionic quasiparticles that have the schematically shown band structure (for $k_z = 0$) of a broad-brimmed Mexican hat. Because of the large DOS at the band edges it is very susceptible to the formation of excitons.

$$H = \sum_{\mathbf{k},\alpha\beta} (d^\dagger_{\mathbf{k},\alpha} \quad f^\dagger_{\mathbf{k},\alpha}) \begin{pmatrix} \epsilon^d_{\mathbf{k}} & \frac{\gamma}{2}\vec{s}_{\mathbf{k}}\vec{\sigma}_{\alpha,\beta} \\ \frac{\gamma}{2}\vec{s}_{\mathbf{k}}\vec{\sigma}_{\alpha,\beta} & \epsilon^f_{\mathbf{k}} \end{pmatrix} \begin{pmatrix} d_{\mathbf{k},\beta} \\ f_{\mathbf{k},\beta} \end{pmatrix} + U \sum_i f^\dagger_{\mathbf{r}_i,\uparrow} f_{\mathbf{r}_i,\uparrow} f^\dagger_{\mathbf{r}_i,\downarrow} f_{\mathbf{r}_i,\downarrow}. \quad (1)$$

The broad Sm d band has a dispersion $\epsilon^d_{\mathbf{k}} = -2t\sum_{\mathbf{k},\eta=x,y,z} \cos k_\eta$. The almost flat inverted f band is $\epsilon^f_{\mathbf{k}} = -\alpha\epsilon^d_{\mathbf{k}} + \lambda$ (with $\alpha \ll 1$) with $\lambda = (1+\alpha)W$ and incorporates the strong on-site repulsion U. The d and f level have different angular momenta and the latter is a superposition of different spin components due to strong spin orbit coupling. Hence, the hybridization in a TKI is spin and momentum dependent (odd parity), $\vec{s}_{\mathbf{k}} = (\sin k_x, \sin k_y, \sin k_z)^T$.

To account for the strongly correlated nature we treat the self-energy of the f electrons as momentum independent such that the main effect of the local repulsion is a renormalization of the f bands and the hybridization [16]. The low energy excitations are described by a new noninteracting Hamiltonian identical to the first term in Eq. (1) but with new parameters $\tilde{t}$ and $\tilde{\gamma}$ [17,18] (we drop the tilde in the remainder). Here, we use effective parameters in agreement with the experimentally known dispersion around the three X points of SmB_6 [19–21].

The Hamiltonian at low temperatures yields two twofold degenerate energies $E^\nu_\pm(\mathbf{k}) = \frac{1}{2}[\epsilon^d_{\mathbf{k}} + \epsilon^f_{\mathbf{k}}] \pm d_{\mathbf{k}}$ with $d_{\mathbf{k}} = \frac{1}{2}\sqrt{(\epsilon^d_{\mathbf{k}} - \epsilon^f_{\mathbf{k}})^2 + |\gamma s_{\mathbf{k}}|^2}$. A schematic form of the band structure is shown in Fig. 1. In the TKI state the lower bands are completely filled and the broad-brimmed Mexican hatlike dispersion gives a large DOS near the gap. For simplicity, we concentrate in the following on an effective two-dimensional model but we have checked that the inclusion of the third dimension does not lead to any qualitative changes of our findings. Setting $k_z = 0$ the Hamiltonian decouples into two independent blocks, labeled by $\nu = +1(-1)$, for the $d^\dagger_\uparrow f_\downarrow$ and $d^\dagger_\downarrow f_\uparrow$ states diagonalized by

$$c_{\mathbf{k},\nu} = \cos\frac{\beta_{\mathbf{k}}}{2} d_{\mathbf{k},\nu} + \sin\frac{\beta_{\mathbf{k}}}{2} e^{i\nu\theta_{\mathbf{k}}} f_{\mathbf{k},\bar{\nu}}$$
$$v_{\mathbf{k},\nu} = -\sin\frac{\beta_{\mathbf{k}}}{2} e^{-i\nu\theta_{\mathbf{k}}} d_{\mathbf{k},\nu} + \cos\frac{\beta_{\mathbf{k}}}{2} f_{\mathbf{k},\bar{\nu}} \quad (2)$$

with the angles given by $\cos\beta_{\mathbf{k}} = (1/2d_{\mathbf{k}})[\epsilon^d_{\mathbf{k}} - \epsilon^f_{\mathbf{k}}]$ and $\sin\beta_{\mathbf{k}} e^{-i\theta_{\mathbf{k}}} = (\gamma/2d_{\mathbf{k}})(\sin k_x - i\sin k_y)$.

Excitons.—To investigate the formation of bound excitons, we include the strong f-level interaction on top of these bands. We project the Hubbard term of Eq. (1) onto the renormalized TKI bands and concentrate only on those terms that lead to exciton binding,

$$H_{\rm int} = -U\sum_{\mathbf{k},\mathbf{k}',\mathbf{q}} [\phi(\mathbf{k}+\mathbf{q},-\mathbf{q})\phi^*(\mathbf{k}'+\mathbf{q},-\mathbf{q}) c^\dagger_{\mathbf{k}+\mathbf{q},-} v_{\mathbf{k},+} v^\dagger_{\mathbf{k}',+} c_{\mathbf{k}'+\mathbf{q},-} + \phi(\mathbf{k},\mathbf{q})\phi^*(\mathbf{k}',\mathbf{q}) v^\dagger_{\mathbf{k}+\mathbf{q},-} c_{\mathbf{k},+} c^\dagger_{\mathbf{k}',+} v_{\mathbf{k}'+\mathbf{q},-}] \quad (3)$$

with $\phi(\mathbf{k},\mathbf{q}) = \sin(\beta_{\mathbf{k}}/2)\cos(\beta_{\mathbf{k}+\mathbf{q}}/2)e^{-i\theta_{\mathbf{k}}}$. Hence, our system is described by the Hamiltonian $H = H_0 + H_{\rm int}$ with $H_0 = \sum_{\mathbf{k},\nu}[E^\nu_+(\mathbf{k})c^\dagger_{\mathbf{k},\nu}c_{\mathbf{k},\nu} + E^\nu_-(\mathbf{k})v^\dagger_{\mathbf{k},\nu}v_{\mathbf{k},\nu}]$ and the valence and conduction bands E^ν_- and E^ν_+ separated by a gap $\Delta = \min(E^\nu_+) - \max(E^\nu_-)$. The interaction only binds electron-hole pairs of opposite ν. For example, $(-+)$ excitons [similarly for the time reversed partner $(+-)$] are created by the operator

$$S^\dagger_{\mathbf{q}} = \sum_{\mathbf{k}} \varphi_{\mathbf{q}}(\mathbf{k}) c^\dagger_{\mathbf{q},-} v_{\mathbf{k}+\mathbf{q},+}, \quad (4)$$

which are directly related to spin flip excitations. We calculate their dispersion $E(\mathbf{q})$ from the Bethe-Salpeter equation

$$[H_0 + H_{\rm int}, S^\dagger_{\mathbf{q}}]|0\rangle = E(\mathbf{q}) S^\dagger_{\mathbf{q}}|0\rangle. \quad (5)$$

We evaluate the quartic operators from the interaction within the ground state, $v^\dagger_{\mathbf{k}}|0\rangle = 0$ and $c_{\mathbf{k}}|0\rangle = 0$, which is equivalent to an Random Phase Approximation (RPA)-type diagrammatic treatment [22]. We obtain a nonlinear equation for the exciton wave function $\varphi_{\mathbf{q}}(\mathbf{k})$ and its dispersion $E(\mathbf{q})$. Because of the fact that the interaction factorizes, as $U\phi(\mathbf{k},\mathbf{q})\phi^*(\mathbf{k}',\mathbf{q})$, this can be cast as a simple implicit equation for $E(\mathbf{q})$,

$$1 = -U\sum_{\mathbf{k}} \frac{|\phi(\mathbf{k},\mathbf{q})|^2}{E(\mathbf{q}) - [E^-_+(\mathbf{k}+\mathbf{q}) - E^+_-(\mathbf{k})]}. \quad (6)$$

We show a representative exciton dispersion in Fig. 2. It has an almost degenerate ringlike manifold of energy

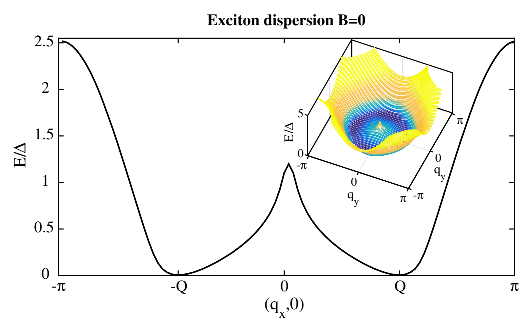

FIG. 2. Shown for $B = 0$ as a function of q_x with $q_y = 0$. The full exciton dispersion of the two-dimensional TKI is plotted in the inset. Because of the special band structure the dispersion minima are always at nonzero momenta but their precise energy depends on the interaction strength. We have used parameters $W = \mu = -3.2$, $\alpha = 0.15$, $\gamma = 0.1$, $U = 2.75$ (in units of hopping t), which give a dispersion with a small gap that can best explain experiments on SmB_6.

minima at momenta $\mathbf{Q}$; see the inset. This peculiar form of the dispersion originates from the special form of the TKI band structure where $\mathbf{Q}/2$ are the vectors pointing to the maxima (minima) of the bands.

In order to account for the anomalies in SmB_6 the exciton binding energy needs to be large such that the exciton gap Δ_{Exc} is small compared to the band gap and sets a low temperature scale. In the simplest approximation excitons can be treated as a noninteracting gas of bosons, with specific heat $C = \sum_{\mathbf{k}} E(\mathbf{k}) \partial n_{\mathbf{k}} / \partial T$ where $n_{\mathbf{k}} = [e^{E(\mathbf{k})/k_B T} - 1]^{-1}$. The almost degenerate ringlike minimum of the excitons has strong consequences for the behavior of experimental observables because it reduces the effective dimensionality to one dimension. For perfect degeneracy and $\Delta_{\mathrm{Exc}} = 0$ such that $E(\mathbf{q}) \propto (|\mathbf{q}| - |\mathbf{Q}|)^2$, it is easy to show that a residual specific heat contribution $C/T \propto 1/\sqrt{T}$ appears independent of dimensionality.

Although it might appear that one must tune $\Delta_{\mathrm{Exc}} \approx 0$ to obtain this interesting low temperature behavior, in fact no such fine-tuning is needed in more realistic models. First, lattice effects lift the degeneracy such that the divergence in specific heat would be removed below a scale Δ_{deg}, which is the difference between the maximum and minimum energy on the ring. Second, Pauli blocking suppresses the formation of excitons with similar momenta. Third, exciton-exciton interactions should be included, and suppress the exciton number. We have modeled the influence of these effects on $n_{\mathbf{k}}$, including exciton-exciton interactions in a self-consistent theory (details are in Supplemental Material [23]). The qualitative low temperature behavior of the free boson approximation survives without any fine-tuning of the parameters; e.g., even for a small negative gap the exciton density remains small.

The resulting specific heat is shown in the upper panel of Fig. 3. Clearly, excitons inside the band gap lead to an extra contribution in contrast to a pure fermionic scenario (black dashed), which has exponential suppression at low T [6]. The main panel shows the specific heat as calculated from the self-consistently determined exciton dispersion compared to the asymptotic behavior of a noninteracting model with $\Delta_{\mathrm{deg}} = 0$ (thin dot dashed) and $\neq 0$ (thin dashed). In the inset of Fig. 3 we show C/T calculated for different values of the exciton gap. We find a strong low temperature exciton contribution with an upturn very similar to experiments on SmB_6 [5,6].

Charge neutral excitons cannot lead to charge transport; however, they can conduct heat. Within a semiclassical Boltzmann-like treatment we calculate their thermal conductivity as $\kappa = \sum_{\mathbf{k}} l_{\mathrm{MFP}} |v_{\mathbf{k}}| E(\mathbf{k}) \partial n_{\mathbf{k}} / \partial T$ with velocity $v_{\mathbf{k}} = \partial E(\mathbf{k}) / \partial \mathbf{k}$ and the mean free path l_{MFP}. Excitons dominate thermal conductivity at temperatures below the charge gap. Their contribution originates again from the special form of the exciton dispersion, e.g., noninteracting bosons with a gapless dispersion with a perfectly degenerate ringlike minimum directly give $\kappa/T = \mathrm{const}$, thus mimicking the behavior of a metal. As shown in the lower panel of

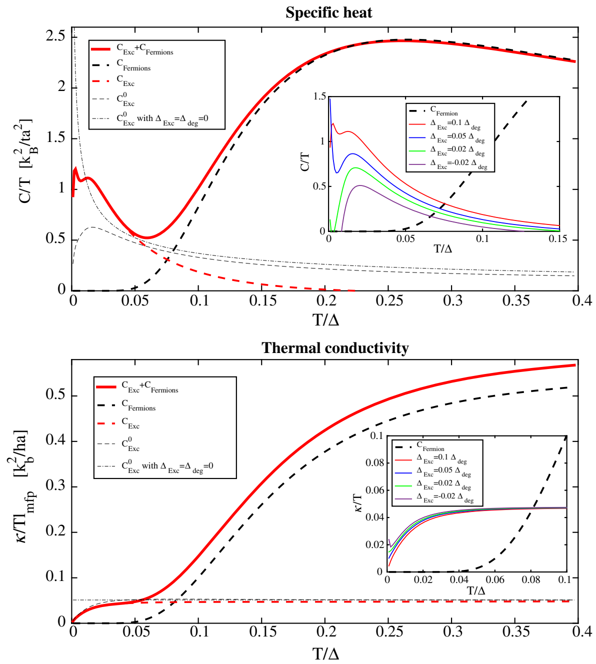

FIG. 3. The upper panel shows the specific heat for $B = 0$, plotted as C/T, as a function of scaled temperature T/Δ with the fermionic band gap Δ. For comparison, we plot the behavior of noninteracting excitons, C^0_{Exc}, with a dispersion with a perfect degenerate ringlike minimum (black dot dashed) or in the self-consistent lattice dispersion (black dashed). We use the same parameters as in the upper panel of Fig. 3 (with $\Delta_{\mathrm{deg}}/\Delta = 1/20$, $\Delta_{\mathrm{Exc}} = \Delta_{\mathrm{deg}}/10$, $g = 0.004t$) and scale the exciton contribution by a factor 1/4. The lower panel shows the thermal conductivity plotted as κ/T.

Fig. 3, in our interacting lattice calculation this linear κ-term is nonzero but strongly reduced for increasing Δ_{Exc}; see the inset. Since the precise value of the exciton gap is sensitive to microscopic details, there may be variations in the asymptotic low temperature behavior between samples [8,32] arising from small changes in this gap.

Magnetoexcitons for $B > 0$.—Already a weak field has direct consequences in our scenario, e.g., the lifting of degenerate exciton branches ($c^\dagger_- v_+$ and $c^\dagger_+ v_-$) from a Zeeman coupling, and a reduction of the fermionic gap, which leads to an increase of the thermal conductivity κ and the specific heat anomaly [33].

But could excitons also lead to a de Haas–van Alphen effect (dHvAE)? Of course, the MEXC itself is charge neutral and its center of mass does not undergo cyclotron motion due to the absence of a Lorentz force [34]. However, they are built of particle and hole bands that form discrete Landau levels (LLs) in a magnetic field that in turn can lead to QO even for band insulators [35,36]. Hence, the energy of the MEXC varies periodically as a function of $1/B$ through the variation of the energy of its constituents. This ultimately simple mechanics (abbreviated as EdHvAE) leads to an oscillatory behavior of the total energy as a function of $1/B$ and hence the magnetization.

The temperature dependence of the EdHvAE can be estimated qualitatively. We have shown recently [35] that narrow gap insulators can exhibit an anomalous dHvAE if the cyclotron frequency $\hbar\omega_c$ is comparable to the activation gap of the insulating state; see also Ref. [36]. SmB_6 has an activation gap of about ≈ 10 meV [14,21] and a small effective mass of the itinerant d band [19,21], $m_d = 0.44 m_e$, leading to $\hbar\omega_c \approx 4$ meV for 15 Tesla. Hence, the $B = 0$ gap is slightly bigger than the cyclotron energy; however, in a TKI the gap is reduced in a magnetic field [36]. Overall, we expect that the amplitude of oscillations from the anomalous dHvAE is small but otherwise follows a Lifshitz-Kosevich temperature dependence [35,36] at higher temperatures. Since the EdHvAE also originates from the periodic variation of gapped LL branches we expect a temperature dependence similar to that of the anomalous dHvAE but with an enhanced intensity.

It is tempting to speculate about the low temperature contribution of MEXC, which is complicated by the appearance of several low energy scales, e.g., $\Delta_{\rm deg}$, $\Delta_{\rm Exc}$. For $\Delta_{\rm Exc} < 0$ a condensate should form at a temperature T^* below which the density of MEXC quickly grows leading to a steeply increasing QO amplitude. A schematic plot of such a temperature dependence is shown in the inset of Fig. 4. For $\Delta_{\rm Exc} > 0$ we would expect a thermally activated number of excitons (and contribution to QO) for $T < \Delta_{\rm Exc}$. However, when projecting the f-level repulsion onto the TKI bands we have only concentrated on those terms that lead to direct exciton binding, but there exist residual terms that create or destroy pairs of $(+-)$ and $(-+)$ excitons. On the one hand, these exciton-nonconserving terms smooth out the condensation transition to a mere crossover. On the other hand, they lead to a correction to the ground state energy from virtual exciton-pair fluctuations, which entails a contribution to the QO amplitude even in the absence of thermally excited excitons for $\Delta_{\rm Exc} > 0$ and $T \to 0$.

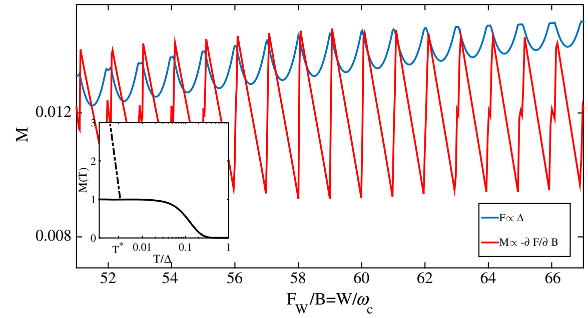

FIG. 4. The energy of MEXC, which is mainly given by the LL gap for weak MEXC binding, changes periodically as a function of inverse magnetic field; see Eq. (7). Therefore, the free energy of the exciton system F (blue) varies periodically together with the corresponding magnetization M (red) (the same parameters as before and $\gamma/W = 0.025$). The schematic temperature dependence is shown in the inset.

We can corroborate our qualitative discussion of the EdHvAE by a microscopic calculation in the strong field limit. Details of our MEXC calculation from Eq. (1) are in Supplemental Material [23]. Similar to the $B = 0$ case, the interaction only binds particle-hole pairs from opposite sectors ν. For a given magnetic field there is a LL index N_- (N_+) such that the energy of the corresponding valence (conduction) LL branch $E_-^{\nu}(N_-)$ $[E_+^{\bar\nu}(N_+)]$ is maximal (minimal). We study the formation of excitons between those extremal levels and obtain a closed expression for the MEXC dispersion,

$$E(\mathbf{k}) = \Delta(B) - U\left(\cos\frac{\beta^-_{N_+}}{2}\right)^2\left(\sin\frac{\beta^+_{N_-}}{2}\right)^2\frac{(-1)^{N_-+N_+-1}}{2\pi}e^{-(k^2/2)}L^{N_--N_++1}_{N_+-1}\left(\frac{k^2}{2}\right)L^{N_+-1-N_-}_{N_-}\left(\frac{k^2}{2}\right) \quad (7)$$

with the LL gap $\Delta(B) = E_+^-(N_+) - E_-^+(N_-)$ and the angles given by $\tan\beta_n^\nu = (\hbar\gamma/2\sqrt{2}l_B)[\sqrt{n}/\hbar\omega_c(n-\nu\frac{1}{2}) + \alpha\hbar\omega_c(n+\nu\frac{1}{2}) - \lambda]$ $(l_B = \sqrt{c\hbar/eB}$, $\omega_c = eB/m_d c)$.

In the regime $E_B < \hbar\omega_c < \Delta(B)$ the change of the exciton dispersion $E(\mathbf{k})$ as a function of field arises mainly from the changing LL gap $\Delta(B)$; see Eq. (7). Then, for a given temperature the free energy and the magnetization are directly related to the periodic variation of the gap $M = -\partial F/\partial B \propto -\partial\Delta/\partial B$. In Fig. 4 we plot this oscillatory behavior as a function of $W/\hbar\omega_c = F_W/B$. There is indeed an exciton contribution to the magnetization whose period $1/F_W$ corresponds to a dHvAE frequency set by the area of the intersection of the unhybridized bands similar to experiments in SmB_6 [7].

Discussion.—Several experiments on SmB_6 have observed in-gap states reminiscent of our excitons. INS measured weakly dispersing spin excitons [9–14] but with a much bigger gap. Scanning tunneling spectroscopy [37] and inelastic light scattering [38] find evidence for collective modes. The notorious resistivity plateau at low temperatures, which was originally attributed to impurity bands [39], has also been related to exciton complexes that acquire charge by trapping electrons [40]. However, transport measurements [41] can relate the plateau to surface states, which invalidates such a polaronic explanation.

In our excitonic scenario we expect that applying a magnetic field should increase C, κ and T^*. To settle the ongoing debate whether the experimentally observed QOs are coming from gapless surface states [34,42,43] or from the bulk [7,35,36], one should directly compare the field dependence of charge transport [Shubnikov–de Haas effect (SdHE)], and thermodynamic quantities (dHvAE). If both were only due to gapless surface states the behaviors of the

SdHE and dHvAE should be similar to those in a metal. However, if one is a bulk signal and the other from the surface we expect that both differ strongly.

There are strong predictions to test our scenario. First, despite the absence of a bulk SdHE there should be QO in the thermal conductivity that would also allow a clear separation of the exciton contribution from phonons. Second, in addition to the observed spin excitons around 10 meV [12–14] we expect another very low energy mode in INS experiments $\lesssim 1$ meV, which so far could have been masked by the quasielastic signal in previous experiments that focused on energies above 5 meV.

In conclusion, we have shown that TKIs are susceptible to the formation of excitons with a ringlike dispersion. They gives rise to a low temperature specific heat contribution, residual thermal conductivity, and an unexpected dHvAE in agreement with observations in SmB_6.

We thank G. Lonzarich and S. Sebastian for helpful discussions and for sharing their experimental data. The work is supported by a fellowship within the postdoctoral program of the German Academic Exchange Service (DAAD) and by the EPSRC Grant No. EP/J017639/1.

*jk628@cam.ac.uk

[1] A. C. Hewson, *The Kondo Problem to Heavy Fermions* (Cambridge University Press, Cambridge, 1993).
[2] A. Menth, E. Buehler, and T. H. Geballe, Magnetic and Semiconducting Properties of SmB_6, Phys. Rev. Lett. **22**, 295 (1969).
[3] M. Dzero, K. Sun, V. Galitski, and P. Coleman, Topological Kondo Insulators, Phys. Rev. Lett. **104**, 106408 (2010).
[4] Liang Fu and C. L. Kane, Topological insulators with inversion symmetry, Phys. Rev. B **76**, 045302 (2007).
[5] J. C. Nickerson, R. M. White, K. N. Lee, R. Bachmann, T. H. Geballe, and G. W. Hull, Jr., Physical properties of SmB_6, Phys. Rev. B **3**, 2030 (1971).
[6] W. A. Phelan, S. M. Koohpayeh, P. Cottingham, J. W. Freeland, J. C. Leiner, C. L. Broholm, and T. M. McQueen, Correlation between Bulk Thermodynamic Measurements and the Low-Temperature-Resistance Plateau in SmB_6, Phys. Rev. X **4**, 031012 (2014).
[7] B. S. Tan, Y.-T. Hsu, B. Zeng, M. C. Hatnean, N. Harrison, Z. Zhu, M. Hartstein, M. Kiourlappou, A. Srivastava, M. D. Johannes, T. P. Murphy, J.-H. Park, L. Balicas, G. G. Lonzarich, G. Balakrishnan, and S. E. Sebastian, Unconventional Fermi surface in an insulating state, Science **349**, 287 (2015).
[8] S. Sebastian and G. Lonzarich (to be published).
[9] P. S. Riseborough, Theory of the dynamic magnetic response of $Ce_3Bi_4Pt_3$: A heavy-fermion semiconductor, Phys. Rev. B **45**, 13984 (1992).
[10] P. S. Riseborough, Collapse of the coherence gap in Kondo semiconductors, Phys. Rev. B **68**, 235213 (2003).
[11] W. T. Fuhrman and P. Nikolic, In-gap collective mode spectrum of the topological Kondo insulator SmB_6, Phys. Rev. B **90**, 195144 (2014).
[12] P. A. Alekseev, J.-M. Mignot, J. Rossat-Mignod, V. N. Lazukov, I. P. Sadikov, E. S. Konovalova, and Y. B. Paderno, Magnetic excitation spectrum of mixed-valence SmB_6 studied by neutron scattering on a single crystal, J. Phys. Condens. Matter **7**, 289 (1995).
[13] P. A. Alekseev, J.-M. Mignot, E. S. Clementyev, V. N. Lazukov, and I. P. Sadikov, Magnetic excitations and variation of valence in SmB_6-based systems, Physica (Amsterdam) **234B**, 880 (1997).
[14] W. T. Fuhrman, J. Leiner, P. Nikolic, G. E. Granroth, M. B. Stone, M. D. Lumsden, L. DeBeer-Schmitt, P. A. Alekseev, J.-M. Mignot, S. M. Koohpayeh, P. Cottingham, W. Adam Phelan, L. Schoop, T. M. McQueen, and C. Broholm, Interaction Driven Subgap Spin Exciton in the Kondo Insulator SmB_6, Phys. Rev. Lett. **114**, 036401 (2015).
[15] V. Alexandrov, P. Coleman, and O. Erten, Kondo Breakdown in Topological Kondo Insulators, Phys. Rev. Lett. **114**, 177202 (2015).
[16] N. Read, D. M. Newns, and S. Doniach, Stability of the Kondo lattice in the large-N limit, Phys. Rev. B **30**, 3841 (1984).
[17] H. Ikeda and K. Miyake, A theory of anisotropic semiconductor of heavy fermions, J. Phys. Soc. Jpn. **65**, 1769 (1996).
[18] M. Legner, A. Regg, and M. Sigrist, Topological invariants, surface states, and interaction-driven phase transitions in correlated Kondo insulators with cubic symmetry, Phys. Rev. B **89**, 085110 (2014).
[19] F. Lu, J. Z. Zhao, H. Weng, Z. Fang, and X. Dai, Correlated Topological Insulators with Mixed Valence, Phys. Rev. Lett. **110**, 096401 (2013).
[20] M. Neupane, N. Alidoust, S.-Y. Xu, T. Kondo, Y. Ishida, D. J. Kim, Chang Liu, I. Belopolski, Y. J. Jo, T.-R. Chang, H.-T. Jeng, T. Durakiewicz, L. Balicas, H. Lin, A. Bansil, S. Shin, Z. Fisk, and M. Z. Hasan, Surface electronic structure of the topological Kondo-insulator candidate correlated electron system SmB_6, Nat. Commun. **4**, 2991 (2013).
[21] E. Frantzeskakis, N. de Jong, B. Zwartsenberg, Y. K. Huang, Y. Pan, X. Zhang, J. X. Zhang, F. X. Zhang, L. H. Bao, O. Tegus, A. Varykhalov, A. de Visser, and M. S. Golden, Kondo Hybridization and the Origin of Metallic States at the (001) Surface of SmB_6, Phys. Rev. X **3**, 041024 (2013).
[22] T. Ando, Excitons in carbon nanotubes, J. Phys. Soc. Jpn. **66**, 1066 (1997).
[23] See Supplemental Material http://link.aps.org/supplemental/10.1103/PhysRevLett.118.096604 for details of the self-consistent theory incorporating exciton-exciton interactions and details of the MEXC calculation, which includes Refs. [24–31].
[24] D. Shoenberg, *Magnetic Oscillations in Metals* (Cambridge University Press, Cambridge, 1984).
[25] I. V. Lerner and Yu. E. Lozovik, Mott exciton in quasitwo-dimensional semiconductors in strong magnetic fields, Zh. Eksp. Teor. Fiz. **78**, 1167 (1980) [Sov. Phys. JETP **51**, 588 (1981)].
[26] Yu. A. Bychkov and E. I. Rashba, Two-dimensional electron-hole system in a strong magnetic field: biexcitons and charge-density waves, Zh. Eksp. Teor. Fiz. **85**, 1826 (1983) [Sov. Phys. JETP **58**, 1062 (1983)].
[27] C. Kallin and B. I. Halperin, Excitations from a filled Landau level in the two-dimensional electron gas, Phys. Rev. B **30**, 5655 (1984).

[28] A. H. MacDonald, Hartree-Fock approximation for response functions and collective excitations in a two-dimensional electron gas with filled Landau levels, J. Phys. C **18**, 1003 (1985).
[29] Yu. A. Bychkov and G. Martinez, Magnetoplasmon excitations in graphene for filling factors $\nu \leq 6$, Phys. Rev. B **77**, 125417 (2008).
[30] C. Toeke and V. I. Fal'ko, Intra-Landau-level magnetoexcitons and the transition between quantum Hall states in undoped bilayer graphene, Phys. Rev. B **83**, 115455 (2011).
[31] K. S. Koelbig and H. Scherb, On a Hankel transform integral containing an exponential function and two Laguerre polynomials, J. Comput. Appl. Math. **71**, 357 (1996).
[32] Y. Xu, S. Cui, J. K. Dong, D. Zhao, T. Wu, X. H. Chen, Kai Sun, Hong Yao, and S. Y. Li, Bulk Fermi Surface of Charge-Neutral Excitations in SmB6 or Not: A Heat-Transport Study, Phys. Rev. Lett. **116**, 246403 (2016).
[33] K. Flachbart, S. Gabni, K. Neumaier, Y. Paderno, V. Pvlik, E. Schuberth, and N. Shitsevalova, Specific heat of SmB_6 at very low temperatures, Physica (Amsterdam) **378B**, 610 (2006).
[34] O. Erten, P. Ghaemi, and P. Coleman, Kondo Breakdown and Quantum Oscillations in SmB_6, Phys. Rev. Lett. **116**, 046403 (2016).
[35] J. Knolle and N. R. Cooper, Quantum Oscillations without a Fermi Surface and the Anomalous de Haas–van Alphen Effect, Phys. Rev. Lett. **115**, 146401 (2015).
[36] L. Zhang, X.-Y. Song, and Fa Wang, Quantum Oscillation in Narrow-Gap Topological Insulators, Phys. Rev. Lett. **116**, 046404 (2016).
[37] W. Ruan, C. Ye, M. Guo, F. Chen, X. Chen, G.-M. Zhang, and Yayu Wang, Emergence of a Coherent In-Gap State in the SmB_6 Kondo Insulator Revealed by Scanning Tunneling Spectroscopy, Phys. Rev. Lett. **112**, 136401 (2014).
[38] P. Nyhus, S. L. Cooper, Z. Fisk, and J. Sarrao, Low energy excitations of the correlation-gap insulator SmB_6: ffA light-scattering study, Phys. Rev. B **55**, 12488 (1997).
[39] J. W. Allen, B. Batlogg, and P. Wachter, Large low temperature Hall effect and resistivity in mixed-valent SmB_6, Phys. Rev. B **20**, 4807 (1979).
[40] S. Curnoe and K. A. Kikoin, Electron self-trapping in intermediate-valent SmB_6, Phys. Rev. B **61**, 15714 (2000).
[41] D. J. Kim, S. Tomas, T. Grant, J. Botimer, Z. Fisk, and Jing Xia, Surface Hall effect and nonlocal transport in SmB_6: Evidence for surface conduction, Sci. Rep. **3**, 3150 (2013).
[42] G. Li, Z. Xiang, F. Yu, T. Asaba, B. Lawson, P. Cai, C. Tinsman, A. Berkley, S. Wolgast, Y. S. Eo, D.-J. Kim, C. Kurdak, J. W. Allen, K. Sun, X. H. Chen, Y. Y. Wang, Z. Fisk, and L. Li, Two-dimensional Fermi surfaces in Kondo insulator SmB_6, Science **346**, 1208 (2014).
[43] A. Thomson and S. Sachdev, Fractionalized Fermi liquid on the surface of a topological Kondo insulator, Phys. Rev. B **93**, 125103 (2016).